D-Garment: Physically Grounded Latent Diffusion for Dynamic Garment Deformations

Anonymous authors
Paper under double-blind review

Abstract

We present a method to dynamically deform 3D garments, in the form of 3D polygon mesh, based on body shape, motion, and physical cloth material properties. Considering physical cloth properties allows to learn a physically grounded model, with the advantage of being more accurate in terms of physically inspired metrics such as strain or curvature. Existing work studies pose-dependent garment modeling to generate garment deformations from example data, and possible data-driven dynamic cloth simulation to generate realistic garments in motion. We propose *D-Garment*, a learning-based approach trained on new data generated with a physics-based simulator. Compared to prior work, our 3D generative model learns garment deformations conditioned by physical material properties, which allows to model loose cloth geometry, especially for large deformations and dynamic wrinkles driven by body motion. Furthermore, the model can be efficiently fitted to observations captured using vision sensors such as 3D point clouds. We leverage the capability of diffusion models to learn flexible and powerful generative priors by modeling the 3D garment in a 2D parameter space, and learning a latent diffusion model using this representation independently from the mesh resolution. This allows to condition global and local geometry with body and cloth material information. We quantitatively and qualitatively evaluate *D-Garment* on both simulations and data captured with a multi-view acquisition platform. Compared to recent baselines our method is more realistic and accurate in terms of shape similarity and physical validity metrics. Code and data will be shared upon acceptance.

1 Introduction

Dressing avatars with dynamic garments is a long-standing challenge in computer graphics and learning-based modeling. Garments are used in virtual applications, ranging from entertainment industries such as video games and animation, to fashion with clothing design and virtual try-on. In applications involving an avatar such as telepresence and virtual change rooms, an important use case is accurately fitting a dynamic garment model to observations captured using vision sensors such as 2D videos, or dynamic 3D point clouds.

We consider the problem of deforming a 3D garment based on physical inputs, via learning a conditional generative model of 3D geometry deformation. Given a garment template mesh, physical parameters of the cloth material, and the wearer's body shape, pose and preceding motion, our method models the distribution over dynamic garment geometries $p(\text{garment deformation} \mid \text{body motion, shape, material})$, and outputs temporally consistent 3D deformations.

Existing work can be categorized into two main classes. Pose-dependent garment models (Vidaurre et al., 2024; De Luigi et al., 2023; Zheng et al., 2024; Shen et al., 2020; Corona et al., 2021) output a garment draped over a body given a characterization of the cloth, a body shape, and a pose. These methods have been successfully tested on downstream tasks such as garment reconstruction from observations and garment retargeting to different users. However, the problem is under-constrained as the 3D geometry of the same garment on the same body performing the same pose can vary depending on the velocity and acceleration of the body parts. Existing work outputs a motion-independent solution, which prevents these methods from generating temporal garment details caused by different dynamics.

In contrast, dynamic cloth simulation methods (Bertiche et al., 2022; Tiwari et al., 2023; Santesteban et al., 2022; Chen et al., 2024; Grigorev et al., 2023) realistically animate dynamic clothes on humans in motion. They produce physically plausible deformations given a garment in rest-pose, body shapes and motions. However, these models leverage cloth motion descriptors to predict the next cloth state. Hence, they are not designed for fitting to observations captured using vision sensors.

To allow for dynamic garments that can be fitted to observations using optimization, we present a physically grounded conditional generative model of 3D garment deformation. We define cloth material as the combination of the three physical quantities bending, stretching and density. To work at high resolution, we take advantage of a latent diffusion model (Ho et al., 2020; Rombach et al., 2022) in a two-dimensional *uv*-space to conditionally deform a fixed garment template. The model provides fine-grained control over input conditions related to the person wearing the garment and the garment's material. The diffusion model defines a distribution over plausible garment deformations, enabling the generation of multiple consistent outputs conditioned on the same input.

To efficiently condition our model on motion and body shape information, we leverage a parametric body model and condition the garment deformation on body shape and a sequence of poses describing the motion. While our model is agnostic to the parametric body model as long as it decouples identity and pose *e.g.* Neophytou & Hilton (2013);

Figure 1: For two different motions (lines) and three varying cloth materials (colors), *D-Garment* uses a latent diffusion model to generate dynamic garment deformations from physical inputs defined by a cloth material and the underlying body shape and motion. Our model can represent large deformations and fine wrinkles.

Pishchulin et al. (2017); Loper et al. (2015); Xu et al. (2020); Mihajlovic et al. (2022), we use SMPL (Loper et al., 2015) as it is easy to integrate. For physical grounding, we condition our model on parameters controlling cloth material by training the model with the output of a physics-inspired simulator. While any physics-inspired simulator that allows controlling material via parameters is applicable *e.g.* Baraff & Witkin (1998); Provot (1995); Narain et al. (2012); Bouaziz et al. (2014); Li et al. (2018a), we use a projective dynamics simulator (Ly et al., 2020) due to computational efficiency and a low number of parameters.

For training and evaluation, we use the physics-based simulator to generate a synthetic dataset of a dynamically deforming wide dress with complex geometry. The dress is simulated using different body shapes, motions, and material parameters. The resulting dataset contains 172 unique body motions from AMASS (Mahmood et al., 2019). Each motion is randomly performed by 3 body shapes and simulated with 3 cloth materials. The sewing pattern of the dress used for simulation was chosen to correspond to a dress in 4DHumanOutfit (Armando et al., 2023), a dataset of reconstructed dressed 3D humans in motion acquired using a multi-view camera platform. This allows for evaluation on acquired data.

We apply our model to a registration task, where we optimize our model's parameters to fit the result to dynamic 3D point cloud sequence of 4DHumanOutfit. We build a two stage pipeline that first fits a parametric body model to the sequence, and subsequently optimizes the latent vector of our model by minimizing the Chamfer distance.

Comparative experiments show that our approach outperforms state-of-the-art baselines in terms of geometric shape fidelity and physically inspired metrics due to its capability of disentangling body motion and cloth material.

In summary, the main contributions of this work are:

- A physically grounded method to dynamically deform a 3D garment to match input cloth materials, body shape and motion, based on a 2D latent diffusion model.

- A dataset of a dynamic 3D dress with a complex sewing pattern simulated for different body shapes, motions and cloth materials. It contains simulated sequences of 172 motions with variations of body shape and cloth material, totaling more than 1500 sequences.

- A registration method fitting our model's parameters to dynamic point cloud sequences of captured dressed humans in motion.

2 Related Work

Dynamic garment modeling is a growing research area in computer vision. Current learning-based models can be categorized into two classes: pose-dependent garment modeling and dynamic cloth simulation. Achar et al. (2024) provide an exhaustive review on cloth draping methods. We focus on works that learn garment models, which in particular excludes works that reconstruct possibly animatable garments.

Pose-Dependent Garment Modeling. Modeling 3D garments is traditionally time-consuming and requires expertise. Data-driven cloth models alleviate this process by enabling parametric 3D modeling and automatic cloth-body draping. These models can be applied to various tasks, such as 3D model reconstruction from images or point clouds. SMPLicit (Corona et al., 2021) is a parametric model capable of generating diverse garments with a fine-grained control over cloth cut and design. Follow-up works modeled diverse garments given different inputs such as image (Sarafianos et al., 2025), 2D masks (Zheng et al., 2024), sketches (Wang et al., 2018) and more recently text (He et al., 2024; Nakayama et al., 2025; Bian et al., 2025). To fit the generated 3D model over different body shapes, a parametric body model (Loper et al., 2015) is commonly used. The garment can be posed using the body's Linear Blend Skinning (LBS) weights. This straightforward approach needs to compute LBS weights of the garment w.r.t. the body and does not model pose-dependent high-frequency details.

Yang et al. (2018) studied cloth deformation across different body poses and motions by analyzing statistics of clothing layer deformations modeled w.r.t. an underlying parametric body model. While this allows to generalize to new factors, the model has limited capacity.

TailorNet (Patel et al., 2020) proposed a scalable model that generalizes across body poses by predicting low and high frequency wrinkles driven by body shape, pose and garment style. DiffusedWrinkles (Vidaurre et al., 2024) leveraged a diffusion model in uv-space to generate wrinkles conditioned like TailorNet. Another line of works (Ma et al., 2020; Laczkó et al., 2024; Shen et al., 2020) models deformations directly over the body surface learning pose-dependent information. DrapeNet (De Luigi et al., 2023) splits the problem into a 3D generative model and a draping model. A recent approach based on point clouds (Ma et al., 2022) learns dynamic LBS weights to model humans in loose clothing but it is not adapted for generative modeling. Shi et al. (2024) built a transformer model capable of synthesizing dynamic garments from body sequences.

Most of these approaches represent static deformations driven by a single pose, omitting dynamic deformations driven by body motion and the physical properties of the garment. Loose garments pose significant challenges due to reliance on either pre-computed LBS weights or deformations defined on the body surface. In contrast, we propose a latent diffusion model conditioned on physics-informed parameters, body pose and motion, enabling the generation of temporally coherent dynamic garments. Our approach is capable of capturing both static and dynamic wrinkles which are traditionally predicted by cloth simulators.

Dynamic Cloth Simulation. Physics-based simulation is a traditional approach in computer graphics for garment animation (Nealen et al., 2006b; Baraff & Witkin, 1998). While state-of-the-art simulators are capable of accurately reproducing cloth dynamics (Li et al., 2018a; Romero et al., 2021), these methods are computationally expensive. Learning-based simulation has been introduced to accelerate computation (Pfaff et al., 2021; Sanchez-Gonzalez et al., 2020; Kairanda et al., 2024). The line of work most closely related to ours focuses on cloth-body interactions to animate dynamic garments over humans (Li et al., 2024; Santesteban et al., 2022; Chen et al., 2024; Grigorev et al., 2023; 2024; Zhang et al., 2022). The use of a parametric body model, instead of a generic rigid-body mesh, allows to predict dynamic deformations from a canonical space leveraging LBS for pose and shape deformations.

Recent works focus on deforming garments in response to body motion. Santesteban et al. (2021) formulated the motion given a current pose and body part velocities and accelerations. SNUG (Santesteban et al., 2022) introduced a self-supervised model to prune computationally expensive data generation. GAPS (Chen et al., 2024) improved SNUG by predicting LBS weights adapted to loose garments. HOOD (Grigorev et al., 2023) built a graph neural network enabling free-flowing motion without relying on LBS for posing. ContourCraft (Grigorev et al., 2024) added new losses to HOOD reducing cloth-body collisions and cloth self-penetration. Motion Guided Deep Dynamic Garments (MGDDG) (Zhang et al., 2022) predicted garment deformations in a generative way given previous states of garment and body.

Note that to achieve consistent cloth dynamics, current learned-based cloth simulation methods leverage previous cloth states either explicitly with vertices velocity (Grigorev et al., 2023; 2024; Zhang et al., 2022) or implicitly using recurrent architecture (Santesteban et al., 2021; 2022; Chen et al., 2024). In contrast, our approach is not auto-regressive, thereby enabling dynamic garment deformations at any given frame facilitating tasks such as fitting to observations.

Positioning. Table 1 positions our work w.r.t. scalable 3D garment models that generalize over body shape and pose. Our work combines advantages of existing works and allows for generalization across materials, dynamic detail modeling, and fitting to observations.

Table 1: Positioning of our work w.r.t. existing learning-based 3D garment models that generalize over multiple body shapes and poses. Our model additionally generalizes across materials, models dynamic details, and allows fitting to observations in the form of dynamic 3D point clouds.

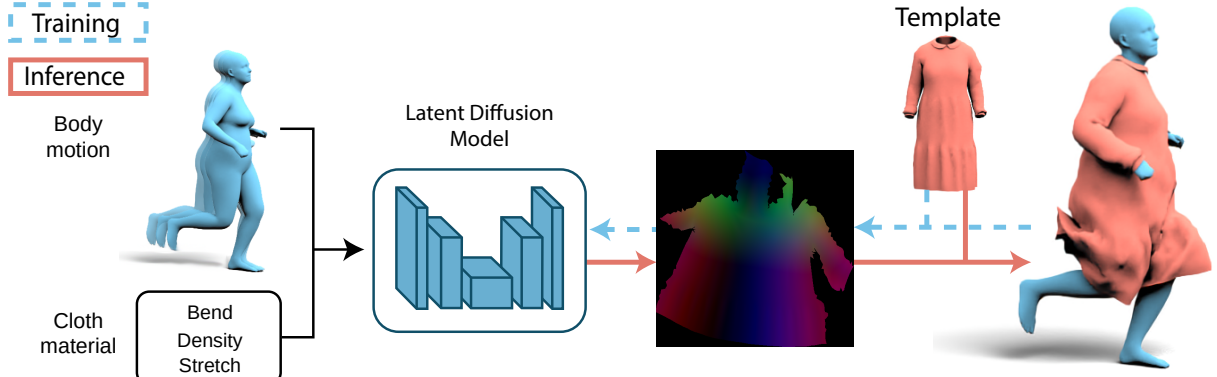|	Generalization across cloth material	Models dynamic details	Allows fitting to observations
Pose-Dependent Garment Modeling			
TailorNet (Patel et al., 2020)			
DiffusedWrinkles (Vidaurre et al., 2024)			✓
Laczkó et al. (2024)			
Cape (Ma et al., 2020)			✓
Shen et al. (2020)	✓		✓
DrapeNet (De Luigi et al., 2023)			✓
SkiRT (Ma et al., 2022)			✓
Shi et al. (2024)		✓	
Dynamic Cloth Simulation			
Santesteban et al. (2021)		✓	
SNUG (Santesteban et al., 2022)		✓	
GAPS (Chen et al., 2024)		✓	
HOOD (Grigorev et al., 2023)	✓	✓	
ContourCraft (Grigorev et al., 2024)	✓	✓	
MGDDG (Zhang et al., 2022)		✓	✓
Ours	✓	✓	✓

Figure 2: *D-Garment* generates garment deformations conditioned on body shape, motion and cloth material. It builds upon a 2D latent diffusion model (Sec. 3.2) to learn how to deform a template in *uv*-space (Sec. 3.1). 3D mesh vertex displacement from template is parameterized by the *uv* displacement map, and our model is trained on it along with the conditional inputs. At inference, our model generates the deformed garment by iteratively denoising the Gaussian noise w.r.t. its conditional inputs.

3 Method

Given a garment template represented as 3D triangle mesh $\mathcal{T}$, our goal is to learn a conditional generative model $\mathcal{G}$, called *D-Garment*, that deforms $\mathcal{T}$ into new mesh instances $\mathcal{M}$ while keeping the mesh topology fixed. We condition the generation on the underlying body shape, pose, pose velocity, and physical material properties of the garment. Conditioning on physical material properties allows to physically ground the model. At test time, *D-Garment* can be used for generation and fitting.

D-Garment represents a dynamic garment on top of a parametric human body model that decouples body shape and pose parameters. In our implementation, we use SMPL (Loper et al., 2015), and represent body shape $\boldsymbol{\beta}$ and pose sequence $\boldsymbol{\theta}_{t-2}, \boldsymbol{\theta}_{t-1}, \boldsymbol{\theta}_t$ as concatenation of the two preceding poses and the current one, where t denotes a discrete time step and $l = 2$ the pose sequence length. The representation of cloth material is inspired by traditional works in physics-inspired simulation (Baraff & Witkin, 1998) and includes stretch coefficient $\mathbf{s}$ (in N/m), mass density coefficient $\mathbf{d}$ (in kg/m^2) and bending coefficient $\mathbf{b}$ (in $N \cdot m$) as $\boldsymbol{\gamma} := [\mathbf{s}, \mathbf{d}, \mathbf{b}]$. Parameter $\mathbf{s}$ controls resistance to stretching or compression, $\mathbf{d}$ controls the influence of inertia, and $\mathbf{b}$ controls resistance to bending or curvature changes. These parameters will be used to physically ground the model.

Inspired by the recent success of diffusion models in 2D domain generation, our 3D mesh generator $\mathcal{G}$ consists of a 2D latent diffusion model, based on the latent diffusion architecture of Rombach et al. (2022). Our model, illustrated in figure Figure 2, directly generates a mesh deformation

$$\mathcal{M}_t \sim \mathcal{G}(\boldsymbol{\theta}_{t-2}, \boldsymbol{\theta}_{t-1}, \boldsymbol{\theta}_t, \boldsymbol{\beta}, \boldsymbol{\gamma}). \tag{1}$$

This formulation is independent of intermediate body-driven skinning, unlike prior works *e.g.* (Patel et al., 2020; Zhang et al., 2022; De Luigi et al., 2023; Vidaurre et al., 2024), which removes the need to rig $\mathcal{T}$.

3.1 Garment Representation

To leverage powerful diffusion models in the 2D domain for generation, we reframe our 3D generation problem by representing garment deformations in a 2D domain encoding (u, v) coordinates. Inspired by *geometry images* from Gu et al. (2002), we encode relative 3D mesh vertex displacements from $\mathcal{T}$ into a 2D geometric displacement map $D := \{d_{i,j}\} \in \mathbb{R}^{n \times m \times 3}$ via a pre-computed *uv* parametrization ϕ of $\mathcal{T}$.

Given an inferred displacement map $\hat{D}$, the inverse uv-map ϕ^{-1} allows to lift pixels to mesh vertices as

$$\hat{\mathcal{M}}^k = \mathcal{T}^k + \hat{d}_{\phi^{-1}(v_k)}, \tag{2}$$

where v_k is the kth vertex in $\mathcal{T}$. Inversely, forward mapping, combined with triangle barycentric coordinate-based interpolation, computes a continuous displacement map for a deformed mesh $\mathcal{M}$ as

$$d_{i,j} = \mathcal{M}^{\phi(i,j)} - \mathcal{T}^{\phi(i,j)}. \tag{3}$$

3.2 Diffusion Model

Using a canonical 2D representation of 3D garment meshes allows to benefit from well established scalable 2D latent diffusion architectures and their pre-trained weights. Being the state-of-the-art in text to image generation, diffusion models have been extended to various applications (Po et al., 2024). The latent diffusion model introduced by Rombach et al. (2022) is made of a variational auto-encoder (VAE) that maps high resolution images to a lower resolution latent space where reverse diffusion is learned based on denoising diffusion probabilistic models (Ho et al., 2020) by a denoising network ϵ_θ. The key strength of diffusion models lies in their reversibility. The forward process involves learning to predict artificially added noise in images. The reverse process, formulated as an iterative refinement, enables the model to gradually remove noise from the latent space, reconstructing high-quality data step by step. We adapt this model to learn generation of geometric displacement maps with conditions that allow for physical grounding.

Training. First, we adapt the VAE of Podell et al. (2024) to our mesh displacement map data distribution $\{\mathcal{M}_t, D_t\}_t$. Since the statistics of this displacement map differs from natural images, pre-trained VAE would be sub-optimal. We finetune the decoder via an extended training loss combining L_2 reconstruction error $||\hat{D} - D||_2$ and the displaced vertex-to-vertex error $||\hat{\mathcal{M}} - \mathcal{M}||_2$. Next, the conditional denoiser ϵ_θ is trained with denoising score matching using samples $\{D_t, \boldsymbol{\theta}_{t-2}, \boldsymbol{\theta}_{t-1}, \boldsymbol{\theta}_t, \boldsymbol{\beta}, \boldsymbol{\gamma}\}_t$ from our training data corpus as

$$\mathbb{E}_{\mathbf{z}, \epsilon, s} \left[||\epsilon - \epsilon_\theta(\mathbf{z}_s, s | \boldsymbol{\theta}_{t-2}, \boldsymbol{\theta}_{t-1}, \boldsymbol{\theta}_t, \boldsymbol{\beta}, \boldsymbol{\gamma})||_2^2 \right], \tag{4}$$

where $\mathbf{z} \in \mathbb{R}^{64 \times 64 \times 4}$ is the latent for D_t, $\epsilon \sim \mathcal{N}(0, I)$, s the diffusion time step, and the noisy latent obtained with forward diffusion $\mathbf{z}_s = \alpha_s \mathbf{z} + \sigma_s \epsilon$. The scaling factor and standard deviation of the forward diffusion are

$$\bar{\alpha}_s = \prod_{u=1}^{s} (1 - \beta_u), \quad \alpha_s = \sqrt{\bar{\alpha}_s}, \quad \sigma_s = \sqrt{1 - \bar{\alpha}_s}, \tag{5}$$

where variance β_u is determined by the noise schedule.

Inference. At test time, a latent Gaussian noise $\mathbf{z}_T$ is iteratively denoised with ϵ_θ to generate a latent displacement map $\mathbf{z}_0$, conditioned on body shape, poses and cloth material. The VAE then decodes $\mathbf{z}_0$ into a displacement map $\hat{D}$, which allows to compute mesh $\hat{\mathcal{M}}$ with Equation (2). Several algorithms can be used to reverse the latent diffusion (*e.g.* DDPM (Ho et al., 2020) or DDIM (Song et al., 2021)) with varying levels of inference speed, sample quality and stochasticity. We use the DPM-Solver++ (Lu et al., 2022) sampler thanks to its quality for the number of denoising steps required.

Fitting. Inspired by a registration method (Guo et al., 2024), we use our model to deform $\mathcal{T}$ to fit observations represented as a 3D point cloud sequence $\mathcal{P}$. As $\mathcal{P}$ typically contains additional points belonging to the body or other garments, we fit our model to $\mathcal{P}$ using Chamfer Distance $\mathcal{L}_{\text{CD}}$ with the adaptive robust function ρ (Barron, 2019), a cloth-body collision loss $\mathcal{L}_c$ and a regularisation loss $\mathcal{L}_{reg}$ consisting in Laplacian smoothing (Nealen et al., 2006a), normal consistency and edge length minimization. This can be viewed as generating sample meshes $\mathcal{M}^*$ that match $\mathcal{P}$, leading to the optimization of the latent $\mathbf{z}_T^*$ as:

$$\mathbf{z}_T^* = \arg \min_{\mathbf{z}_T} \rho \left(\mathcal{L}_{\text{CD}}(\mathcal{P}, \mathcal{M}^*) \right) + \mathcal{L}_c + \mathcal{L}_{reg}, \tag{6}$$

where $\mathcal{M}^*$ is generated in a differentiable way through our sampler from a latent $\mathbf{z}_T^*$, conditioned on $\boldsymbol{\gamma}$ and the body motion $\boldsymbol{\beta}, \boldsymbol{\theta}_i$'s. The latent $\mathbf{z}_T^*$ is optimized with Adam (Kingma & Ba, 2014).

Inspired by the clothing energy term in Yang et al. (2016), $\mathcal{L}_c$ is defined as:

$$\mathcal{L}_c = \sum_{v \in \mathcal{M}^*} \delta_{\text{in}}(v, \mathcal{B}) \min_{b \in \mathcal{B}} ||v - b||_2, \tag{7}$$

where δ_{in} is an indicator function for points inside a mesh, and $\mathcal{B}$ contains the body mesh vertices.

4 Dataset

Prior works often use datasets containing tight garments, with little dynamic effects. To test our approach, we created a dataset of a simulated 3D loose dress. We use a design approaching one of the outfits in 4DHumanOutfit (Armando et al., 2023), allowing to test our model on multi-view reconstructions of a real dress. The dress is simulated over 172 motion sequences, performing walking and running motions from AMASS (Mahmood et al., 2019). For each sequence, three body shapes were uniformly sampled following $\beta \sim \mathcal{U}(-1, 1)$, where $\mathcal{U}$ is a uniform distribution. Furthermore, for each sequence, three cloth materials (bending $\mathbf{b}$, stretching $\mathbf{s}$, density $\mathbf{d}$) were also uniformly sampled following $\gamma \sim \mathcal{U}([10^{-8}, 10^{-4}], [40, 200], [0.01, 0.7])$. Each sequence was simulated for all combinations of the sampled parameters.

Simulation. We used a simulator based on projective dynamics (Ly et al., 2020) which is less physically accurate but 10 times faster than implicit solvers. It also only requires a single value for each cloth material parameter: bending, stretching, density. Other simulation parameters, which does not only depend of the cloth (friction, air damping, collision tolerance), were fixed across all sequences. The simulation frame rate was set to 50 fps. To initialize the simulation, the garment size was manually draped over the canonical body model, avoiding any intersection. Then, the garment was simulated over 100 frames, linearly interpolating from the zero pose and shape to the first frame of the sequence. It was then stabilized over 100 frames to reduce noisy motion.

Data cleaning. SMPL can contain self-intersections, which cause unsolvable cloth-body intersections for the simulator. To solve this, we pre-processed AMASS using an optimization used in Tzionas et al. (2016) to minimize self-penetration. We optimized for body joints that are the most disruptive in simulation *i.e.* arms and shoulders. Angular velocity of poses and the distance to the initial poses were also minimized to regularize the output and maintain temporal consistency. We post-processed simulated cloth sequences with few remaining cloth-body intersections by pushing vertices outside following the nearest body normal. Some simulation failures have been manually removed from the dataset.

5 Experiments

Implementation details. We implemented the inverse uv mapping ϕ^{-1} using bi-linear interpolation. We found that the interpolation technique (*e.g.* nearest, bi-linear or bi-cubic interpolation) is marginally impacting the mesh quality thanks to our high resolution image (512x512). By averaging texture coordinates that correspond to a single mesh vertex, we did not notice any discontinuity on the surface geometry across seams. To avoid remaining collision artifacts, the vertices are pushed outside the body mesh in a simple post-processing step ablated in Table 3.

We used a pretrained VAE from SDXL (Podell et al., 2024) downscaling the images to latents as $\mathbb{R}^{512 \times 512 \times 3} \rightarrow \mathbb{R}^{64 \times 64 \times 4}$. The decoder part was finetuned on $40k$ steps and then frozen during ϵ_θ training. The denoiser network ϵ_θ was built with an U-net (Ronneberger et al., 2015) that takes the encoded latents to 5 convolutional layers of output channel size $(64, 128, 256, 512, 512)$ and conditions via cross-attention (Vaswani et al., 2017). The following conditional input dimensions were used: $\gamma \in \mathbb{R}^3$, $\beta \in \mathbb{R}^8$, $\theta \in \mathbb{R}^{111}$ using 6 dimensional rotations (Zhou et al., 2019) of 18 body joints and a global translation. Both decoder and ϵ_θ weights were optimized using AdamW optimizer (Loshchilov & Hutter, 2019). We have trained ϵ_θ on 50 epochs using a batch size of 32 lasting 10 days on a single NVidia A6000. The noising schedule was set to a cosine variance (Lin et al., 2024) increasing from $\beta_1 = 10^{-4}$ to $\beta_T = 0.02$ sampled in 1000 diffusion steps during training and 20 steps during inference using SDE-DPM++ (Lu et al., 2022). The inference achieves

an interactive frame rate of 7.5 fps. We have used the Diffusers (von Platen et al., 2022) library to implement the diffusion model and PyTorch3D (Ravi et al., 2020) for the regularization loss $\mathcal{L}_{reg}$.

5.1 Evaluation Protocol

Dataset. The garment geometry and body poses are normalized according to the current body global rotation and translation for each frame. The template $\mathcal{T}$ is the mean geometry of the normalized dataset. We compute its *uv* parametrization using OptCuts (Li et al., 2018b) which jointly minimizes the distortion and the seam lengths, limiting under-sampling and discontinuities induced by seams.

We keep 3 motions from AMASS unseen during training for testing, namely "*C19-runtohoptowalk*", "*B16-walkturnchangedirection*" and "*B17-walktohoptowalk1*", and combine them with 3 variations of body shape and cloth material. Note that this test set only comprises data with a combination of unseen motion, unseen body shape and unseen cloth material, which allows to evaluate how well models generalize. We randomly leave out 5% of the remaining training data for evaluation purposes.

Metrics. We quantitatively compare the geometric shape fidelity of the results to the test set with common 3D computer vision metrics. Vertex error E_v shows the accuracy between the prediction and the ground truth. Chamfer euclidean distance E_{CD} assesses the shape similarity of the prediction and the ground truth. Chamfer normal distance E_n allows to compare the wrinkling between the prediction and the ground truth. Nearest vertices corresponding normals are compared using absolute cosine similarity. Latter, we note U the set of uniformly sampled points over the mesh surface $\mathcal{M}$.

$$E_v = \frac{1}{|\mathcal{M}|} \sum_{v \in \mathcal{M}} ||v - \hat{v}||, \qquad E_{CD} = \frac{1}{|U|} \sum_{v \in U} \min_{\hat{v} \in \hat{U}} ||\hat{v} - v|| + \frac{1}{|\hat{U}|} \sum_{\hat{v} \in \hat{U}} \min_{v \in U} ||\hat{v} - v||,$$

These shape similarity metrics allow to estimate how well a method produces similar deformations compared to the simulator. However, they fail to evaluate the physical quality. To address this limitation, we propose several physically inspired metrics inspired by Santesteban et al. (2022). The cloth-body collision percentage E_c measures the amount of clothing predicted inside the body. Higher values indicate physically implausible clothing or simulation failure. Wrinkling error E_b, related to bending **b**, compares dihedral angles to the ground truth. Area strain error E_s, related to stretching **s**, compares the in-plane deformation from the rest shape to the ground truth. The center of mass distance E_d, related to material density **d**, compares the global rigid motion to the ground truth. Note that E_b, E_s and E_d are independent of each other providing a measure of isolated characteristics.

$$E_c = \frac{100}{|U|} \sum_{v \in U} \delta_{\text{in}}(v, \mathcal{B}), \qquad E_b = \sqrt{\frac{1}{|E|} \sum_{e \in E} (\Theta(e) - \Theta(\hat{e}))^2}, \qquad E_s = |\Psi_s(\mathcal{M}) - \Psi_s(\hat{\mathcal{M}})|,$$

where E is the mesh $\mathcal{M}$ set of edges, $\Theta(e)$ computes the signed dihedral angle between adjacent faces, $\Psi_s(\mathcal{M})$ is the integral area strain deformation from the rest pose.

5.2 Comparative Evaluation to Baselines

We compare *D-Garment* to methods that allow for generalization across cloth materials and that model dynamic details. While one of the first approaches allowing for varying motions falls in this category (Yang et al., 2018), this method does not decouple the influence of multiple factors at once due to its limited capacity. For this reason, we compare to the three strong baselines MGDDG (Zhang et al., 2022), HOOD (Grigorev et al., 2023) and ContourCraft (Grigorev et al., 2024). MGDDG is trained on a sequence of 175 frames at 50 fps containing walking and running. The training uses the code provided by MGDDG. HOOD's training on diverse garments generalizes well to our dress without the need of fine-tuning its original pretrained model. ContourCraft is based on HOOD with additional losses to overcome self-collisions. To align timings across methods with varying framerates, we measure all metrics at 10 fps.
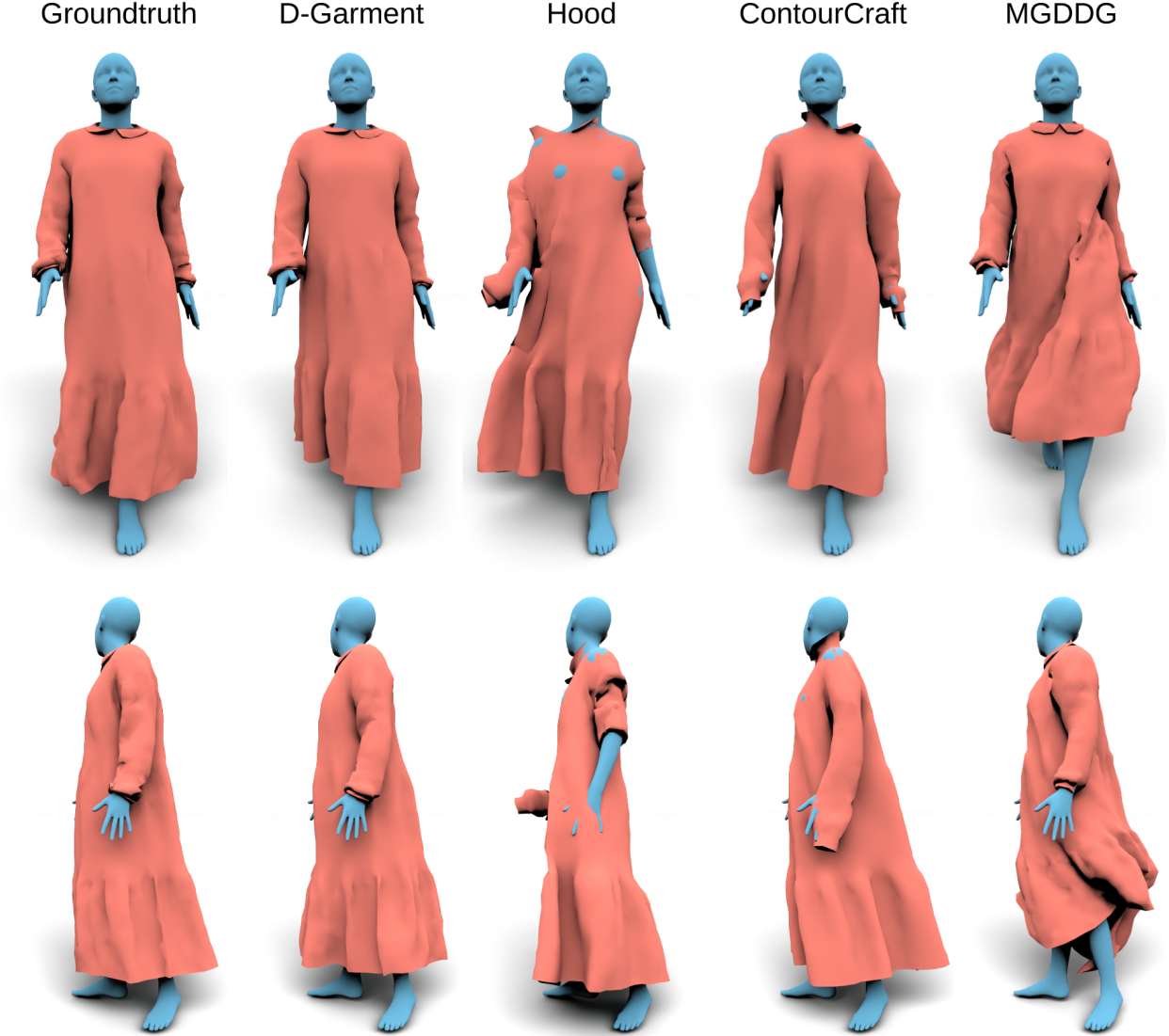
Figure 3: We qualitatively compare *D-Garment* to HOOD (Grigorev et al., 2023), ContourCraft (Grigorev et al., 2024) and MGDDG (Zhang et al., 2022). *D-Garment* generates visually plausible wrinkles without requiring cloth velocity or position input. Corresponding video can be viewed in the supplementary material.

Table 2: Quantitative comparison to HOOD (Grigorev et al., 2023), ContourCraft (Grigorev et al., 2024) and MGDDG (Zhang et al., 2022). Best scores are in **bold**.

	Shape Similarity			Physical Validity			
	E_v	E_{CD}	E_n	E_c	E_b	E_s	E_d
HOOD	19.7510	2.5257	0.6156	1.7956	0.8275	7.6536	14.8808
ContourCraft	9.7465	0.3776	0.5268	1.0819	0.6967	7.5901	6.3436
MGDDG	8.5144	0.3389	0.5592	0.9638	0.8067	31.2323	4.2763
D-Garment	**4.9447**	**0.1863**	**0.4525**	**0.7180**	**0.5951**	**7.0201**	**2.3384**

Figure 4: Varying one cloth material parameter at a time. The model provides control over bending, stretching and density. For each parameter, the color map shows per-vertex distances between minimal and maximal values. 0 ▬▬ 10 cm
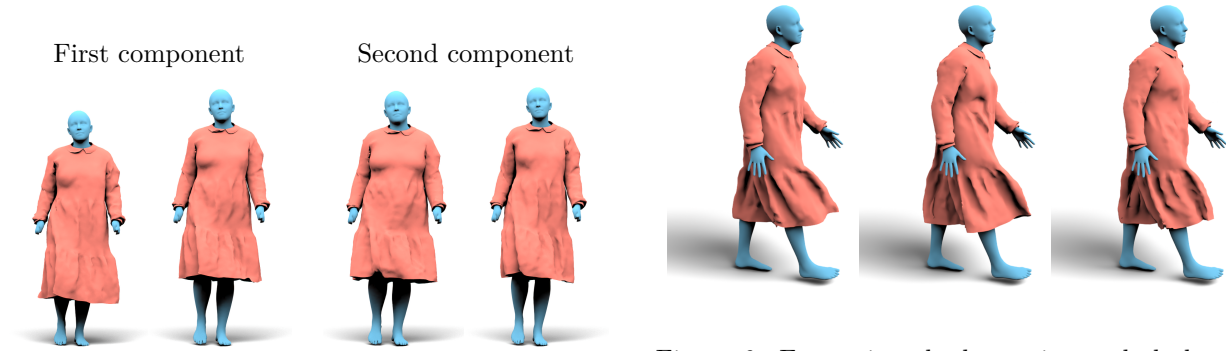

Figure 5: Results for variations of body shape. Our method adapts the garment to the body morphology.
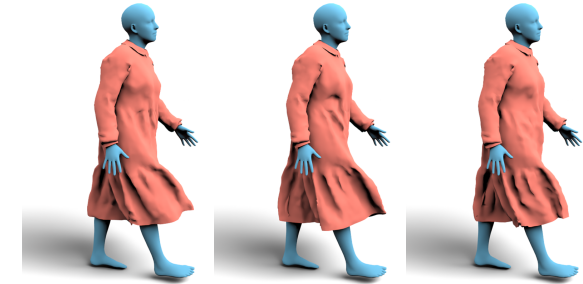

Figure 6: For a given body motion and cloth material, our method can generate subtle yet plausible variations, by varying (from left to right) the random latent noise of the diffusion model.

Table 3: Ablation study w.r.t. different conditioning and processing strategies. Best scores are in **bold**.

	Shape Similarity			Physical Validity			
	E_v	E_{CD}	E_n	E_c	E_b	E_s	E_d
w/o material	7.0097	0.2421	0.4740	**0.6677**	0.6341	8.6457	3.5387
w/o motion	5.2396	0.1985	0.4576	0.7087	0.6013	8.4377	2.3849
w/o post process	4.9589	0.1888	0.4583	1.3632	**0.5839**	7.2277	**2.3163**
w/ subdivision	-	**0.1854**	0.4585	0.8145	-	11.1532	2.3414
D-Garment	**4.9447**	0.1863	**0.4525**	0.7180	0.5951	**7.0201**	2.3384

D-Garment outperforms all baselines in terms of all metrics in Table 2. As all examples in the test set concern unseen motion, unseen body shape and unseen cloth material, Table 2 shows that *D-Garment* provides state-of-the-art results for unseen generation tasks across different cloth material and body motion.

Figure 3 shows a visual comparison to HOOD, ContourCraft and MGDDG simulated on a body motion. The results of *D-Garment* are visually closer to the ground truth simulation. HOOD is struggling to handle pleats around the collar and the wrists because its assumption of a flat surface rest shape. ContourCraft shows less intersections than HOOD but suffers from the same limitations. MGDDG's results are visually pleasing but do not follow the expected material behaviour. More visual results are provided in supplementary material.

5.3 Ablation Study

We perform ablations on the input parameters of the model, the mesh subdivision and the post-processing technique in Table 3. For material and motion ablations, we remove γ and θ in the input vector of ϵ_θ,

respectively, and train the full model. The motion ablation keeps the current pose but omits the prior ones which indicate body velocity. The full model outperforms all ablations in most metrics. *D-Garment* can benefit from the post-processing reducing collision artifacts from 1.3% to 0.7% of intersecting vertices with a marginal physical quality trade-off. Variations in mesh resolution have a negligible impact on the deformed shape, demonstrating the robustness of the *uv* representation. Note that E_v and E_b are not applicable on meshes with different topology, while the physical validity metrics E_c and E_s are sensitive to changes in topology.

Next, we study the influence of material parameters and body shape in the *D-Garment* outputs. Figures 4 and 5 show results for extreme parameter values used during training. Figure 4 keeps all inputs constant while only varying a single cloth material parameter at a time. Note that each parameter influences the resulting geometry of the dress by subtly changing wrinkling patterns. This allows to generate a rich set of results by controlling cloth material. Figure 5 shows results when keeping all inputs constant while only changing a single parameter of the body shape β, along the first two principal components. Note that the same dress is draped on different morphologies, while adapting its shape.

Figure 6 shows results obtained for the same conditions using different random noise for each latent. *D-Garment* allows for high variability, while staying in the space of plausible dynamics.

5.4 Garment fitting to 3D observations

We apply our method to fit temporally consistent garments on humans captured using multi-view videos, represented as sequence of unstructured 3D point clouds. This task presents challenges as the input data is noisy, and the points represent the human wearer in addition to the garment.

Using a recent method Toussaint et al. (2024), we first reconstruct point clouds of the multi-view dataset 4DHumanOutfit (Armando et al., 2023). We then fit a human motion prior (Marsot et al., 2022), modeled as a discrete set of SMPL parameters, to the reconstructed point clouds for each sequence. The body fitting process uses a one-sided Chamfer loss, manually placed landmarks distances and the clothing energy E_{cloth} from Yang et al. (2016) enforcing the body shape to stay inside the capture. Points in the capture are filtered for the cloth fitting process by removing points that are near undressed body parts (feet, legs, hands and head) and isolating the largest cluster of points. We test two material optimization strategies. The first uses fixed material parameters γ initialized to values with minimal constraints $(10^{-8}, 200, 0.01)$. The second strategy optimizes γ by optimizing γ^* in addition to $\mathbf{z}_T^*$ in Equation (6). We optimize for a single input latent of our model following Section 3.2 to fit generated garments to point cloud sequences.

Figure 7 shows a qualitative result for two of the sequences of 4DHumanOutfit (Armando et al., 2023). The input point cloud is shown in blue, and the fitted garment in orange. Visual results indicate that *D-Garment* can robustly recover the garment from dynamic 3D point clouds. Figure 8 shows quantitative results of the fitting application on these two sequences. We measure distances from vertices of *D-Garment* fittings to their nearest neighbors on reconstructed frames of the capture. All fitting results achieve an accuracy inferior to $2.4cm$ on 90% of garment vertices. A distance of $2.4cm$ between our result and the input point cloud is small compared to the highly dynamic garment motions present in 4DHumanOutfit. Furthermore, the error is overestimated for some parts as the dress model is complete, while the reconstructions in 4DHumanOutfit are missing parts due to occlusions in some frames, as shown in Appendix A, where the lower arm and parts of the torso are not reconstructed. Note that *D-Garment* fitting results achieve high accuracy despite this domain gap. Optimizing for material parameters allows for smoother fitted results with a slight loss in surface to target distance.

6 Conclusion

This paper presented *D-Garment*, a 3D dynamic garment deformation model based on a 2D latent diffusion model enabling temporally consistent generation given the body shape, pose, motion and cloth material. The model was learned on a dataset of garments with physical grounding by conditioning the result on cloth material parameters. Both the code and dataset will be made available. Experimental evaluations on both simulated and real data confirm the versatility of *D-Garment* for diverse tasks while providing state-of-the-

art results. These findings highlight the potential of diffusion-based generative models to realistically deform 3D dynamic garments, as well as solving the challenging task of extracting garments from 3D point cloud observations.

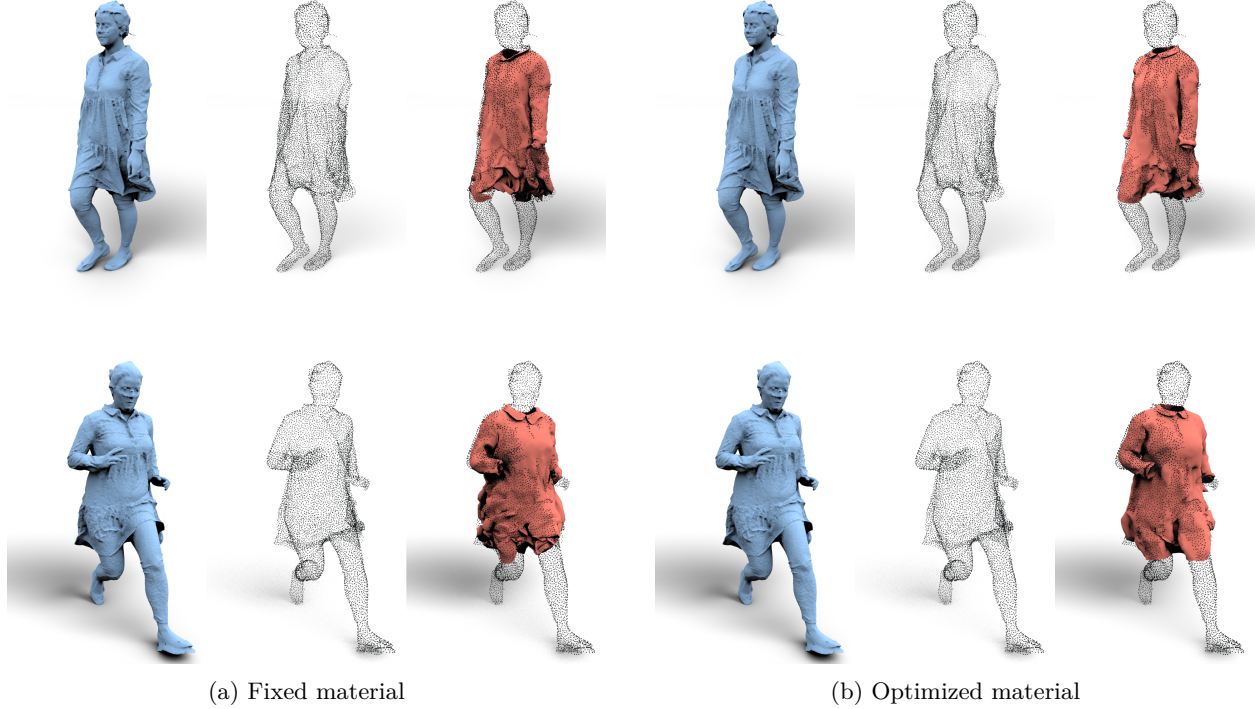(a) Fixed material   (b) Optimized material

Figure 7: *D-Garment* is used to fit a captured 3D sequence. For each time frame of the corresponding motion (lines), we show the raw capture (left blue), the sampled point cloud (middle grey), and the estimated garment (right orange). We can accurately recover garment pose and fine wrinkles using two different material optimization strategies a and b. Corresponding videos are in supplementary material.

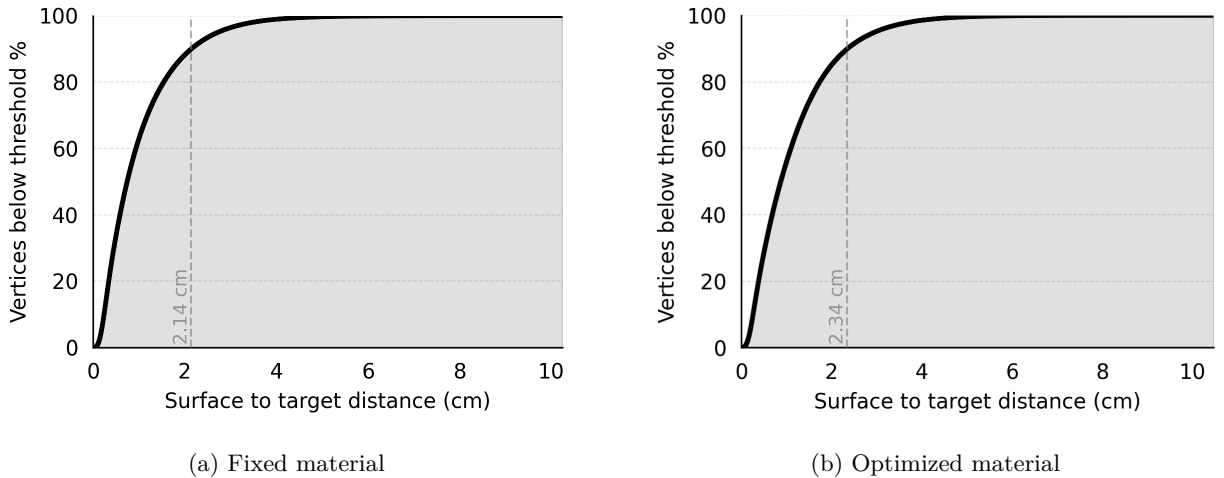(a) Fixed material   (b) Optimized material

Figure 8: Cumulative distances of *D-Garment* fittings to input 3D point clouds for two sequences of 4DHumanOutfit with different material optimization strategies a and b. The vertical bar indicates the maximum distance at 90% of the vertices.

References

Prerana Achar, Mayank Patel, Anushka Mulik, Neha Katre, Stevina Dias, and Chirag Raman. A comparative study of garment draping techniques. *arXiv preprint arXiv:2405.11056*, 2024. 3

Matthieu Armando, Laurence Boissieux, Edmond Boyer, Jean-Sébastien Franco, Martin Humenberger, Christophe Legras, Vincent Leroy, Mathieu Marsot, Julien Pansiot, Sergi Pujades, Rim Rekik Dit Nekhili, Grégory Rogez, Anilkumar Swamy, and Stefanie Wuhrer. 4DHumanOutfit: a multi-subject 4D dataset of human motion sequences in varying outfits exhibiting large displacements. *Computer Vision and Image Understanding*, 237, December 2023. doi: 10.1016/j.cviu.2023.103836. URL https://inria.hal.science/hal-04129186. 2, 7, 11, 17

David Baraff and Andrew Witkin. Large steps in cloth simulation. In *SIGGRAPH*, pp. 767–778, 1998. 2, 4, 5

Jonathan T Barron. A general and adaptive robust loss function. In *Proceedings of the IEEE/CVF conference on computer vision and pattern recognition*, pp. 4331–4339, 2019. 6

Hugo Bertiche, Meysam Madadi, and Sergio Escalera. Neural cloth simulation. *ACM Transactions on Graphics*, 41 (6):1–14, 2022. 2

Siyuan Bian, Chenghao Xu, Yuliang Xiu, Artur Grigorev, Zhen Liu, Cewu Lu, Michael J Black, and Yao Feng. Chatgarment: Garment estimation, generation and editing via large language models. *In Conference on Computer Vision and Pattern Recognition (CVPR)*, 2025. 3

Sofien Bouaziz, Sebastian Martin, Tiantian Liu, Ladislav Kavan, and Mark Pauly. Projective dynamics: fusing constraint projections for fast simulation. *ACM Transactions on Graphics*, 33(4), 2014. 2

Ruochen Chen, Liming Chen, and Shaifali Parashar. Gaps: Geometry-aware, physics-based, self-supervised neural garment draping. In *International Conference on 3D Vision*, pp. 116–125, 2024. 2, 4

Enric Corona, Albert Pumarola, G. Alenyà, Gerard Pons-Moll, and Francesc Moreno-Noguer. Smplicit: Topology-aware generative model for clothed people. *Conference on Computer Vision and Pattern Recognition*, pp. 11870–11880, 2021. 1, 3

Luca De Luigi, Ren Li, Benoît Guillard, Mathieu Salzmann, and Pascal Fua. Drapenet: Garment generation and self-supervised draping. In *Conference on Computer Vision and Pattern Recognition*, pp. 1451–1460, 2023. 1, 3, 4, 5

Artur Grigorev, Michael J. Black, and Otmar Hilliges. HOOD: hierarchical graphs for generalized modelling of clothing dynamics. In *Conference on Computer Vision and Pattern Recognition*, 2023. 2, 4, 8, 9

Artur Grigorev, Giorgio Becherini, Michael Black, Otmar Hilliges, and Bernhard Thomaszewski. Contourcraft: Learning to resolve intersections in neural multi-garment simulations. In *ACM SIGGRAPH 2024 Conference Papers*, pp. 1–10, 2024. 4, 8, 9

Xianfeng Gu, Steven J Gortler, and Hugues Hoppe. Geometry images. In *Conference on Computer Graphics and Interactive Techniques*, pp. 355–361, 2002. 5

Jingfan Guo, Fabian Prada, Donglai Xiang, Javier Romero, Chenglei Wu, Hyun Soo Park, Takaaki Shiratori, and Shunsuke Saito. Diffusion shape prior for wrinkle-accurate cloth registration. In *International Conference on 3D Vision*, pp. 790–799, 2024. 6

Kai He, Kaixin Yao, Qixuan Zhang, Jingyi Yu, Lingjie Liu, and Lan Xu. Dresscode: Autoregressively sewing and generating garments from text guidance. *ACM Transactions on Graphics*, 43(4), 2024. 3

Jonathan Ho, Ajay Jain, and Pieter Abbeel. Denoising diffusion probabilistic models. *Advances in Neural Information Processing Systems*, 33:6840–6851, 2020. 2, 6

Navami Kairanda, Marc Habermann, Christian Theobalt, and Vladislav Golyanik. Neuralclothsim: Neural deformation fields meet the thin shell theory. In *Neural Information Processing Systems (NeurIPS)*, 2024. 4

Diederik P Kingma and Jimmy Ba. Adam: A method for stochastic optimization. *arXiv preprint arXiv:1412.6980*, 2014. 6

Hunor Laczkó, Meysam Madadi, Sergio Escalera, and Jordi Gonzalez. A generative multi-resolution pyramid and normal-conditioning 3d cloth draping. In *Winter Conference on Applications of Computer Vision*, pp. 8709–8718, 2024. 3, 4

Jie Li, Gilles Daviet, Rahul Narain, Florence Bertails-Descoubes, Matthew Overby, George E. Brown, and Laurence Boissieux. An implicit frictional contact solver for adaptive cloth simulation. *ACM Transactions on Graphics*, 37 (4), 2018a. 2, 4

Minchen Li, Danny M. Kaufman, Vladimir G. Kim, Justin Solomon, and Alla Sheffer. Optcuts: joint optimization of surface cuts and parameterization. *ACM Transactions on Graphics*, 37(6), 2018b. 8

Peizhuo Li, Tuanfeng Y Wang, Timur Levent Kesdogan, Duygu Ceylan, and Olga Sorkine-Hornung. Neural garment dynamics via manifold-aware transformers. In *Computer Graphics Forum*, pp. e15028. Wiley Online Library, 2024. 4

Shanchuan Lin, Bingchen Liu, Jiashi Li, and Xiao Yang. Common diffusion noise schedules and sample steps are flawed. In *Winter Conference on Applications of Computer Vision*, pp. 5404–5411, 2024. 7

Matthew Loper, Naureen Mahmood, Javier Romero, Gerard Pons-Moll, and Michael J. Black. Smpl: a skinned multi-person linear model. *ACM Transactions on Graphics*, 34(6), 2015. 2, 3, 5

Ilya Loshchilov and Frank Hutter. Decoupled weight decay regularization. In *International Conference on Learning Representations*, 2019. URL https://openreview.net/forum?id=Bkg6RiCqY7. 7

Cheng Lu, Yuhao Zhou, Fan Bao, Jianfei Chen, Chongxuan Li, and Jun Zhu. Dpm-solver++: Fast solver for guided sampling of diffusion probabilistic models. *arXiv:2206.00927*, 2022. 6, 7

Mickaël Ly, Jean Jouve, Laurence Boissieux, and Florence Bertails-Descoubes. Projective Dynamics with Dry Frictional Contact. *ACM Transactions on Graphics*, 39(4), 2020. 2, 7

Qianli Ma, Jinlong Yang, Anurag Ranjan, Sergi Pujades, Gerard Pons-Moll, Siyu Tang, and Michael J. Black. Learning to Dress 3D People in Generative Clothing. In *Computer Vision and Pattern Recognition*, 2020. 3, 4

Qianli Ma, Jinlong Yang, Michael J Black, and Siyu Tang. Neural point-based shape modeling of humans in challenging clothing. In *International Conference on 3D Vision*, pp. 679–689, 2022. 3, 4

Naureen Mahmood, Nima Ghorbani, Nikolaus F. Troje, Gerard Pons-Moll, and Michael J. Black. AMASS: Archive of motion capture as surface shapes. *International Conference on Computer Vision*, pp. 5441–5450, 2019. 2, 7

Mathieu Marsot, Stefanie Wuhrer, Jean-Sebastien Franco, and Anne Hélène Olivier. Representing motion as a sequence of latent primitives, a flexible approach for human motion modelling. *arXiv preprint arXiv:2206.13142*, 2022. 11

Marko Mihajlovic, Shunsuke Saito, Aayush Bansal, Michael Zollhoefer, and Siyu Tang. COAP: Compositional articulated occupancy of people. In *Conference on Computer Vision and Pattern Recognition*, 2022. 2

Kiyohiro Nakayama, Jan Ackermann, Timur Levent Kesdogan, Yang Zheng, Maria Korosteleva, Olga Sorkine-Hornung, Leonidas Guibas, Guandao Yang, and Gordon Wetzstein. Aipparel: A large multimodal generative model for digital garments. *In Conference on Computer Vision and Pattern Recognition (CVPR)*, 2025. 3

Rahul Narain, Armin Samii, and James F. O'Brien. Adaptive anisotropic remeshing for cloth simulation. *ACM Transactions on Graphics*, 31:1 – 10, 2012. 2

Andrew Nealen, Takeo Igarashi, Olga Sorkine, and Marc Alexa. Laplacian mesh optimization. In *International Conference on Computer Graphics and Interactive Techniques*, pp. 381–389, 2006a. 6

Andrew Nealen, Matthias Müller, Richard Keiser, Eddy Boxerman, and Mark Carlson. Physically based deformable models in computer graphics. *Computer Graphics Forum*, 25(4):809–836, 2006b. doi: https://doi.org/10.1111/j. 1467-8659.2006.01000.x. URL https://onlinelibrary.wiley.com/doi/abs/10.1111/j.1467-8659.2006.01000. x. 4

Alexandro Neophytou and Adrian Hilton. Shape and pose space deformation for subject specific animation. In *International Conference on 3D Vision*, pp. 334–341, 2013. 2

Chaitanya Patel, Zhouyingcheng Liao, and Gerard Pons-Moll. Tailornet: Predicting clothing in 3d as a function of human pose, shape and garment style. *Conference on Computer Vision and Pattern Recognition*, pp. 7363–7373, 2020. 3, 4, 5

Tobias Pfaff, Meire Fortunato, Alvaro Sanchez-Gonzalez, and Peter W. Battaglia. Learning mesh-based simulation with graph networks. In *International Conference on Learning Representations*, 2021. 4

Leonid Pishchulin, Stefanie Wuhrer, Thomas Helten, Christian Theobalt, and Bernt Schiele. Building statistical shape spaces for 3d human modeling. *Pattern Recognition*, 67:276–286, 2017. 2

Ryan Po, Wang Yifan, Vladislav Golyanik, Kfir Aberman, Jonathan T Barron, Amit Bermano, Eric Chan, Tali Dekel, Aleksander Holynski, Angjoo Kanazawa, et al. State of the art on diffusion models for visual computing. In *Computer Graphics Forum*, volume 43, pp. e15063. Wiley Online Library, 2024. 6

Dustin Podell, Zion English, Kyle Lacey, Andreas Blattmann, Tim Dockhorn, Jonas Müller, Joe Penna, and Robin Rombach. SDXL: Improving latent diffusion models for high-resolution image synthesis. In *International Conference on Learning Representations*, 2024. 6, 7

Xavier Provot. Deformation constraints in a mass-spring model to describe rigid cloth behaviour. In *Graphics Interface*, pp. 147–147, 1995. 2

Nikhila Ravi, Jeremy Reizenstein, David Novotny, Taylor Gordon, Wan-Yen Lo, Justin Johnson, and Georgia Gkioxari. Accelerating 3d deep learning with pytorch3d. *arXiv:2007.08501*, 2020. 8

Robin Rombach, Andreas Blattmann, Dominik Lorenz, Patrick Esser, and Bjorn Ommer. High-resolution image synthesis with latent diffusion models. In *Conference on Computer Vision and Pattern Recognition*, 2022. 2, 5, 6

Victor Romero, Mickaël Ly, Abdullah Haroon Rasheed, Raphaël Charrondière, Arnaud Lazarus, Sébastien Neukirch, and Florence Bertails-Descoubes. Physical validation of simulators in computer graphics: A new framework dedicated to slender elastic structures and frictional contact. *ACM Transactions on Graphics*, 40(4):1–19, 2021. 4

Olaf Ronneberger, Philipp Fischer, and Thomas Brox. U-net: Convolutional networks for biomedical image segmentation. In *Medical image computing and computer-assisted intervention*, pp. 234–241, 2015. 7

Alvaro Sanchez-Gonzalez, Jonathan Godwin, Tobias Pfaff, Rex Ying, Jure Leskovec, and Peter Battaglia. Learning to simulate complex physics with graph networks. In *International conference on machine learning*, pp. 8459–8468. PMLR, 2020. 4

Igor Santesteban, Nils Thuerey, Miguel A Otaduy, and Dan Casas. Self-supervised collision handling via generative 3d garment models for virtual try-on. In *Conference on Computer Vision and Pattern Recognition*, pp. 11763–11773, 2021. 4

Igor Santesteban, Miguel A Otaduy, and Dan Casas. Snug: Self-supervised neural dynamic garments. In *Conference on Computer Vision and Pattern Recognition*, pp. 8140–8150, 2022. 2, 4, 8

Nikolaos Sarafianos, Tuur Stuyck, Xiaoyu Xiang, Yilei Li, Jovan Popovic, and Rakesh Ranjan. Garment3DGen: 3d garment stylization and texture generation. In *International Conference on 3D Vision*, 2025. 3

Yu Shen, Junbang Liang, and Ming C Lin. Gan-based garment generation using sewing pattern images. In *European Conference on Computer Vision*, pp. 225–247, 2020. 1, 3, 4

Min Shi, Wenke Feng, Lin Gao, and Dengming Zhu. Generating diverse clothed 3d human animations via a generative model. *Computational Visual Media*, 10(2):261–277, 2024. doi: 10.1007/s41095-022-0324-2. URL https://www.sciopen.com/article/10.1007/s41095-022-0324-2. 3, 4

Jiaming Song, Chenlin Meng, and Stefano Ermon. Denoising diffusion implicit models. In *International Conference on Learning Representations*, 2021. URL https://openreview.net/forum?id=St1giarCHLP. 6

Lokender Tiwari, Brojeshwar Bhowmick, and Sanjana Sinha. GenSim: Unsupervised generic garment simulator. In *Conference on Computer Vision and Pattern Recognition*, pp. 4169–4178, 2023. 2

Briac Toussaint, Laurence Boissieux, Diego Thomas, Edmond Boyer, and Franco Jean-Sébastien. Millimetric Human Surface Capture in Minutes. In *SIGGRAPH Asia*, 2024. 11

Dimitrios Tzionas, Luca Ballan, Abhilash Srikantha, Pablo Aponte, Marc Pollefeys, and Juergen Gall. Capturing hands in action using discriminative salient points and physics simulation. *International Journal of Computer Vision*, 118(2):172–193, 2016. 7

Ashish Vaswani, Noam Shazeer, Niki Parmar, Jakob Uszkoreit, Llion Jones, Aidan N Gomez, Łukasz Kaiser, and Illia Polosukhin. Attention is all you need. *Advances in neural information processing systems*, 30, 2017. 7

Raquel Vidaurre, Elena Garces, and Dan Casas. Diffusedwrinkles: A diffusion-based model for data-driven garment animation. In *British Machine Vision Conference*, 2024. 1, 3, 4, 5

Patrick von Platen, Suraj Patil, Anton Lozhkov, Pedro Cuenca, Nathan Lambert, Kashif Rasul, Mishig Davaadorj, Dhruv Nair, Sayak Paul, William Berman, Yiyi Xu, Steven Liu, and Thomas Wolf. Diffusers: State-of-the-art diffusion models. https://github.com/huggingface/diffusers, 2022. 8

Tuanfeng Y. Wang, Duygu Ceylan, Jovan Popović, and Niloy J. Mitra. Learning a shared shape space for multimodal garment design. *ACM Transactions on Graphics*, 37(6), 2018. 3

Hongyi Xu, Eduard Gabriel Bazavan, Andrei Zanfir, Bill Freeman, Rahul Sukthankar, and Cristian Sminchisescu. GHUM & GHUML: Generative 3d human shape and articulated pose models. In *Conference on Computer Vision and Pattern Recognition*, pp. 6184–6193, 2020. 2

Jinlong Yang, Jean-Sébastien Franco, Franck Hétroy-Wheeler, and Stefanie Wuhrer. Estimation of human body shape in motion with wide clothing. In *European Conference on Computer Vision*, pp. 439–454, 2016. 7, 11

Jinlong Yang, Jean-Sebastien Franco, Franck Hetroy-Wheeler, and Stefanie Wuhrer. Analyzing clothing layer deformation statistics of 3d human motions. In *European Conference on Computer Vision*, 2018. 3, 8

Meng Zhang, Duygu Ceylan, and Niloy J. Mitra. Motion guided deep dynamic 3d garments. *ACM Transactions on Graphics*, 41(6), 2022. 4, 5, 8, 9

Jiali Zheng, Rolandos Alexandros Potamias, and Stefanos Zafeiriou. Design2Cloth: 3d cloth generation from 2d masks. In *Conference on Computer Vision and Pattern Recognition*, pp. 1748–1758, 2024. 1, 3

Yi Zhou, Connelly Barnes, Jingwan Lu, Jimei Yang, and Hao Li. On the continuity of rotation representations in neural networks. In *Conference on Computer Vision and Pattern Recognition*, pp. 5745–5753, 2019. 7

A   Appendix: dress template and capture

Figure 9: The dress model (left) used for *D-Garment* dataset differs slightly from the captured dress (right) from 4DHumanOutfit (Armando et al., 2023) in terms of length and wrinkle details.